

Transducer Placement Option for Ultrasonic Lamb Wave Structural Health Monitoring (SHM) on Damage Tolerant Aircraft Substructure

Ewald, Vincentius; Groves, Roger; Benedictus, Rinze

Publication date

2017

Document Version

Final published version

Published in

Structural Health Monitoring 2017: Real-Time Material State Awareness and Data-Driven Safety Assurance - Proceedings of the 11th International Workshop on Structural Health Monitoring, IWSHM 2017

Citation (APA)

Ewald, V., Groves, R., & Benedictus, R. (2017). Transducer Placement Option for Ultrasonic Lamb Wave Structural Health Monitoring (SHM) on Damage Tolerant Aircraft Substructure. In F. K. Chang, & F. Kopsaftopoulos (Eds.), *Structural Health Monitoring 2017: Real-Time Material State Awareness and Data-Driven Safety Assurance - Proceedings of the 11th International Workshop on Structural Health Monitoring, IWSHM 2017* (Vol. 2, pp. 1811-1818). Destech publications.

Important note

To cite this publication, please use the final published version (if applicable). Please check the document version above.

Copyright

Other than for strictly personal use, it is not permitted to download, forward or distribute the text or part of it, without the consent of the author(s) and/or copyright holder(s), unless the work is under an open content license such as Creative Commons.

Takedown policy

Please contact us and provide details if you believe this document breaches copyrights. We will remove access to the work immediately and investigate your claim.

See discussions, stats, and author profiles for this publication at: <https://www.researchgate.net/publication/319016906>

Transducer Placement Option for Ultrasonic Lamb Wave Structural Health Monitoring (SHM) on Damage Tolerant Aircraft Substructure

Conference Paper · September 2017

DOI: 10.12783/shm2017/14063

CITATION

1

READS

219

3 authors:



Vincentius Ewald

Delft University of Technology

9 PUBLICATIONS 27 CITATIONS

[SEE PROFILE](#)



Roger M Groves

Delft University of Technology

215 PUBLICATIONS 1,059 CITATIONS

[SEE PROFILE](#)



R. Benedictus

Delft University of Technology

300 PUBLICATIONS 4,342 CITATIONS

[SEE PROFILE](#)

Some of the authors of this publication are also working on these related projects:



Gilt Leather Artefacts [View project](#)



SHM based on Time Reversal of Lamb Waves [View project](#)

Transducer Placement Option for Ultrasonic Lamb Wave Structural Health Monitoring (SHM) on Damage Tolerant Aircraft Substructure

Vincentius EWALD¹, Roger GROVES¹, Rinze BENEDICTUS²

ABSTRACT

In this paper, we review two transducer placement options to locate and quantify damage in primary aircraft structures using ultrasonic Structural Health Monitoring (SHM). The first placement approach concerns a known expected damage location, for example a fatigue crack growth from rivet hole. The location of such a damage can already be predicted by fracture mechanics and therefore the focus of this SHM system design is to determine the damage size. For this approach, we have developed our previous work in finite-element (FE) modelling of a damage tolerant aluminum fuselage by introducing an artificial crack into the structural FE model and assessed its influence on the Lamb wave propagation. Image processing was performed by subtracting the wave propagation image of the damaged from the undamaged structure.

A second category of damage occurs at locations that cannot be predicted by fracture mechanics, such as impact damage from hail. This type of damage requires the SHM system to both locate and assess the size of the damage and this is heavily influenced by the positioning of the transducers. Optimal sensor placement (OSP) techniques tend to rely on assessment using the probability of detection (POD) parameter. In this work, we propose an alternative placement method which maximizes the detectability of the transducer coverage area based on the pulse-echo technique without relying on the POD parameter, by determining the fitness function based on sensor coverage area for single and multiple sensors and random damage locations. Results from both these approaches are compared in this paper, with a perspective towards the overall design of SHM systems.

1). Vincentius Ewald, Roger M Groves. Aerospace Non-Destructive Testing Laboratory, Delft University of Technology, Netherlands; Corresponding Email: V.Ewald@tudelft.nl | R.M.Groves@tudelft.nl

2). Rinze Benedictus. Structural Integrity and Composites Group, Faculty of Aerospace Engineering, Delft University of Technology, Netherlands

INTRODUCTION

Sensor Positioning for Lamb Wave SHM

Lamb waves are one of the promising SHM techniques due to their capability to propagate many meters [1, 2]. For damage monitoring, the technique relies on the interaction between the Lamb wave and the damage [3]. At damage locations, Lamb waves are scattered, reflected, absorbed, diffracted, and subject to mode conversion and the change in the received signal can be calculated as a damage indicator (DI). The most commonly used sensor in ultrasonic SHM is a piezoelectric transducer (PZT), which is generally attached to the surface of the structure, thus making sensor placement tremendously important since the DI quantification heavily relies on the sensor placement.

According to [4], a structure designed using the damage tolerance principle is safe to operate until a critical damage threshold is reached. Because a Lamb wave can interact with damage which has a size at least the half of its wavelength [5, 6], and this critical damage tolerant threshold is generally larger than the wavelength, it is safe to assume that a Lamb wave can interact with the critical damage. The task of sensor placement in SHM is therefore to ensure that 1). the interaction between the damage and the wave is sufficient and 2). the location of the sensor enables the capture of this wave – damage interaction.

Literature Overview and Objective

Sensor placement options (SPO) have been previously described, for example prioritizing the sensor location based on the detectability limit [7], the modal analysis parameter for damage localization on a truss structure [8], and by using a global search and greedy algorithm [9]. Haynes [10] proposed sensor placement by minimizing Bayesian cost and thus selected a locally optimal sensor location. However, if the damage occurs outside of that area, it might fail to detect it.

In a more recent study, Thiene et al. [11] introduced DI-free sensor placement optimization based on a fitness function that maximizes the coverage area of the sensor network. Venkat et al. [12] used a Finite Element (FE) simulation platform to build differential images between undamaged and damaged structure. The summed-up energy captured by all sensors were plotted to determine the optimal sensor location from the highest captured energy.

From the above-mentioned articles, we summarized that two SPO streams exist: 1). predictable damage location approach, and 2). random damage location approach. Given the current state of the art of SPO, the objectives of this article are: 1). to generalize the current techniques of both approaches, 2). to propose an alternative DI parameter for the known damage location approach, and 3). to propose the maximization of sensor coverage area by the pulse-echo method.

THEORY

Lamb Wave Propagation

The theoretical analysis of wave propagation in metallic materials, composite, and hybrid materials is described in [13 – 15]. The elastodynamic wave equation in an anisotropic inhomogeneous medium in a bounded domain $\Omega \subset \mathbb{R}^d$ ($d = 2, 3$ for 2- and 3-dimensional cases, respectively) is given in Eq. (1), where $u(x, t)$ is the time and space dependent displacement, ρ material density, C_{ijkl} material stiffness tensor, ε_{kl} strain tensor, and $f(x, t)$ source function, respectively, with $i, j, k,$ and l being the standard notations in the generalized Hooke's law. After applying boundary conditions of two parallel surfaces, there are two solutions to Eq. (1) for wave propagation in homogeneous material of given density, which are well-known as symmetrical modes (S0, S1, S2...) and asymmetrical modes (A0, A1, A2...) [16], respectively.

$$\rho \frac{\partial^2 u(x, t)}{\partial t^2} - \nabla \cdot \left(\sum_{k=1}^d \sum_{l=1}^d C_{ijkl} \varepsilon_{kl} \right) = f(x, t) \quad (1)$$

FE Simulation of Lamb Wave Interaction with Material Inhomogeneities

The FE formulation for Lamb wave propagation is based on Hamilton's principle [17] and this is described in Eq. (4), where Γ and Φ are the surficial and volumetric integral areas, u and \ddot{u} are the particle displacement vectors in the material and their corresponding accelerations, and ε is the strain tensor. The external forces can be classified as surface load F_S and volume load F_V . To numerically solve Eq. (2), the geometry involved is divided into mesh elements over which the equation can be approximated, where the numerical stability of time integration is ensured by the Courant-Friedrich-Lewy (CFL) condition [18].

$$0 = \left(- \int_{\Phi} \left[\rho \cdot \delta \underline{u}^T \cdot \ddot{\underline{u}} + \delta \varepsilon^T \cdot C_{ijkl} \cdot \underline{\underline{\varepsilon}} \right] d\Phi \right) + \left(\int_{\Phi} \left(\delta \underline{u}^T \cdot F_V \right) d\Phi + \int_{\Gamma} \left(\delta \underline{u}^T \cdot F_S \right) \right) \quad (2)$$

Damage Detection Approach: Pulse-Echo vs. Pitch-Catch Technique

In the pulse-echo technique, the transducer acts both as a sensor and actuator, and the coverage area is circular, while the resulting area in the pitch-catch configuration is elliptical (Fig. 1). The disadvantage of this pulse-echo technique is that the localization of the damage becomes less precise in comparison to the pitch-catch technique. Nevertheless, the performance of the pulse-echo method can be

improved by utilizing multiple sensors. The further investigations in this paper are with the pulse-echo technique.

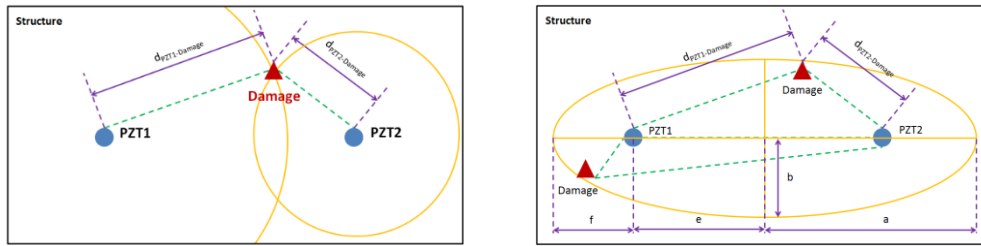


Figure 1: Coverage area of pulse-echo technique (left) and pitch-catch technique (right). The distance between sensor and damage is marked by $d_{PZT-Damage}$, while a , b , e , f are the ellipse parameters

METHODOLOGIES

SPO Approach for Predictable Damage Location by Numerical Simulation

For a damage tolerant design, fracture mechanics is used predict the most probable damage location under a certain loading condition [19]. A damage will most likely appear in an area with higher local stress intensity factor (SIF). By knowing the most probable damage location and the critical damage size for a certain geometry, two FE simulations scenarios of Lamb wave propagation can be performed: 1). in an undamaged structure and 2). in a critically damaged structure. An example of these scenarios is depicted in Fig. 2a-d.

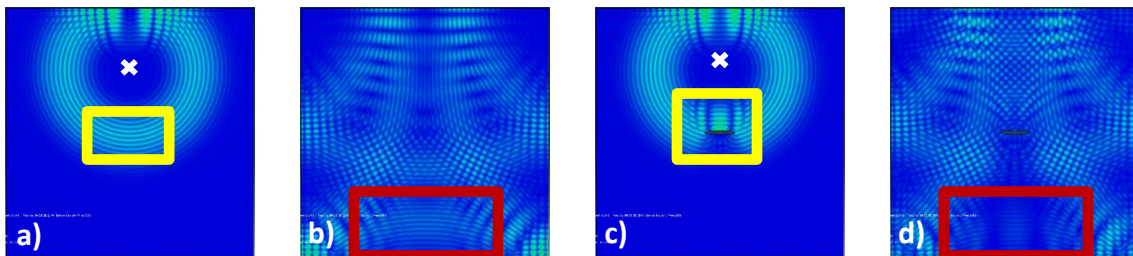


Figure 2: Lamb Wave propagation in a). healthy structure at 20 μ s, b). healthy structure at 60 μ s, c). damaged structure at 20 μ s, d). damaged structure at 60 μ s. The ultrasonic pulse is excited at $t = 0 \mu$ s from the point 'x'. The yellow and red rectangles are regions of interest referenced in the text.

In Fig. 2a-d, Lamb wave propagation in an aluminum plate with a size of 160x160x1 mm was simulated using ABAQUS FE software. To ensure calculation accuracy, a quadratic brick element (C3D20) was used and the global mesh size was kept at 1 mm³, resulting in around 25000 elements. One can clearly see from Fig. 2a and 2c by comparing the regions in the yellow squares, that at $t = 20 \mu$ s the propagation was partially interrupted at the crack front and a part of the wave has been reflected. As the wave is continuously propagating in time and space, the

wave pattern is also changing every time increment, as depicted in the red squares in Fig. 2b and 2d. Differential images of wave scatter can be created from those images. More on this processing can be found in results and discussion section.

SPO Approach for Random Damage Location by Pulse-Echo Technique

For an unpredictable damage location such as an impact, the time-dependent wave scatter image approach is hardly useful since it requires too many simulations. In this case, we define the sensor coverage area as the circular area in which all pixels are covered within the distance between PZT and the damage. Fig. 3a depicts an example of a single PZT in the random damage scenario in simplified square structure represented by 10 x 10 pixels. A damage which is close to the PZT will result in smaller coverage area (blue pixels in Fig. 3b). The further the damage is located from the PZT, the larger coverage area will be (red pixels in Fig. 3c).

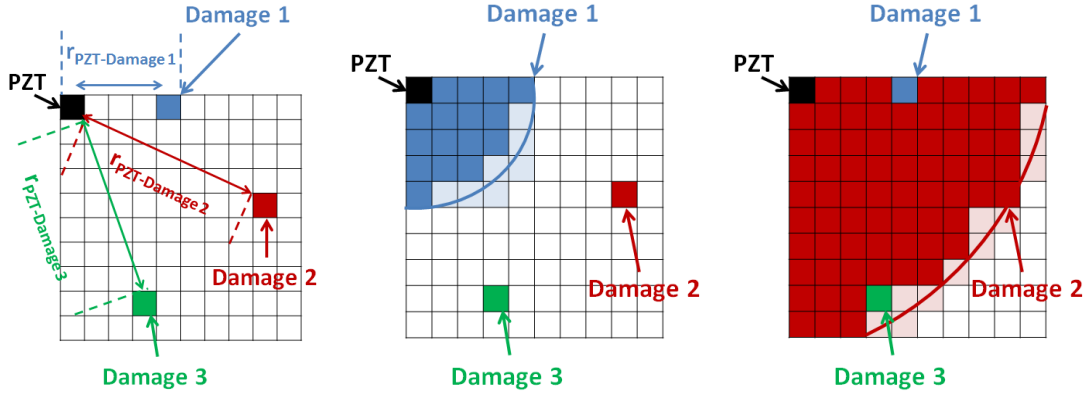


Figure 3a: Scenario with 3 random damages
Figure 3b: Area covered between PZT and Damage 1
Figure 3c: Area covered between PZT and Damage 2

There are two main wave attenuations during Lamb wave propagation: 1). attenuation due to a geometric barrier (e.g. rivet holes or step thickness) and 2). a frequency attenuation factor due to material properties. Even without geometric spreading, an attenuation by material properties will always take place. Thus we define the target function f which represents the coverage area A at pixel $p(x_i, y_j)$ as

$$f(x_i, y_j) = \alpha \cdot \ln(A) \cdot \exp\left(\frac{\beta}{r}\right) \quad (5)$$

In Eq. (5), α is the attenuation parameter due to geometric spreading in an area A which is measured from the distance between the PZT and the pixel, and β is the frequency attenuation factor [20] which increases if the excitation frequency is increased. By calculating f for all pixels, the total score TS for a certain sensor position S at pixel $p_S(x_i, y_j)$ in the structure with a geometric barrier B at pixel

$p_B(x_m, y_n)$ is defined in Eq. (6). The sensor coverage can then be mapped as a function of the pixel coordinate.

$$TS(x_i, y_j) = \sum_S f_S(x_i, y_j) - \sum_B f_B(x_m, y_n) \quad (6)$$

RESULTS AND DISCUSSION

Differential Images of Wave Scatter with Blob Analysis

Differential images of the wave scatter are depicted in Fig. 4a-d, where the green pixels are increased signal and the magenta pixels are reduced signals due the crack. MATLAB has quick and ready-to-use blob detection algorithm in the image processing toolbox, which was used for the analysis. The images were first converted into 256 greyscales (see Fig.5a-d), and the area of the non-white pixels (either the increased or reduced wave portion) are detected as blobs whose boundaries are marked by red polygons and whose centroid can be calculated. Each centroid of the blobs can be calculated. Physically, these centroids correspond to the averaged changes in the wave scatter and accordingly, to maximize damage detectability a PZT sensor should be placed at the centroid coordinates.

In Fig. 5a-d, the largest centroid is marked by the red dot, the second largest by the green dot, and the remaining centroids by the blue dots. The coordinates of the largest centroids are given by Table 1. The scaling is 4.81 pixels per cm. In later work, we plan to develop an algorithm which combines the centroid coordinates from all time frames to assess the variation of the crack angle on the detectability.

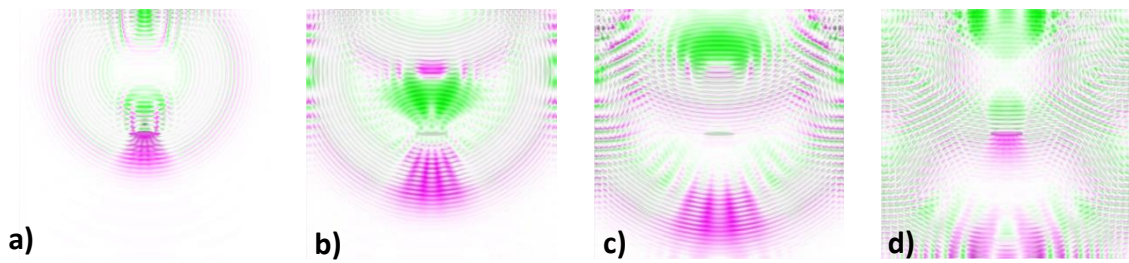


Figure 4: Differential images of wave scatter at a). $t = 20 \mu s$, b). $t = 30 \mu s$, c). $t = 40 \mu s$, and d). $t = 50 \mu s$

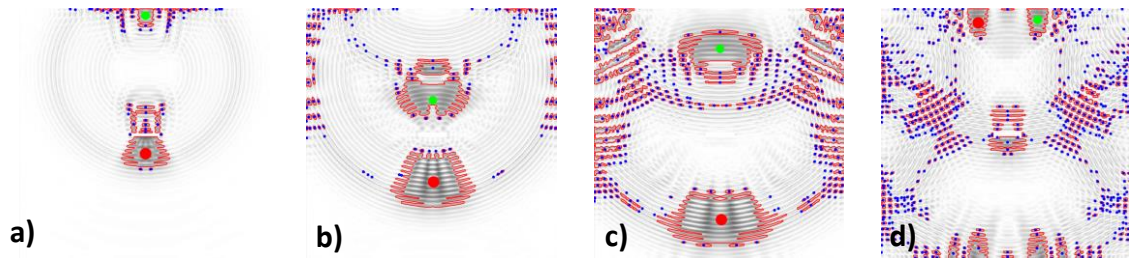


Figure 5: Detected blobs in Fig. 4a-d, where the red dot is the largest centroid, the green dot is the second largest centroid, and the blue dots are the remaining centroids

Time frame	Largest centroid		Second-largest centroid	
	[pixel]	[cm]	[pixel]	[cm]
30 μ s	(385,443)	(80.0,92.1)	(385,22)	(80.0,4.6)
40 μ s	(388,529)	(80.7,110.0)	(386,280)	(80.2,58.2)
50 μ s	(389,644)	(80.9,133.9)	(385,123)	(80.0,25.6)
60 μ s	(296,44)	(61.5,9.1)	(476,35)	(99.0,7.3)

Table 1: (X,Y) – Coordinates of the largest and second largest centroid in pixels and in cm

Sensor Coverage Score Mapping

As a demonstration of the total score mapping in Eq. (5), a flat plate with dimensions of 80 cm x 50 cm was modelled. The spatial resolution was 1 cm², so there are 4000 pixels in total. By calculating the target function f from Eq. (5) for every pixel, a coverage map can be built. As an example, sensor placement at coordinate (x|y = 40|25 cm) gives the coverage map depicted in Fig. 6, where the area closer to the PZT is marked by blue to green color indicating a higher f -value, thus better damage detectability and the area further from the PZT has reduced damage detectability, which is marked by yellow to red color.

This approach was extended to the riveted lap joint with multiple rivet holes depicted by Fig. 7. The plate has the same dimension as previously mentioned and sensors were placed at (x|y = 10|25 cm) and (x|y = 70|25 cm). In this plate, several rivet holes exist and their coordinates are (x|y = 50|5 cm ; 50|15 cm ; 50|25 cm ; 50|35 cm ; 50|45 cm ; 60|5 cm ; 60|15 cm ; 60|25 cm ; 60|35 cm ; 60|45 cm). Also Fig. 7 shows that area closer to the PZT is marked by a blue to green color, while the area surrounding the rivet holes is marked by an orange to red color. The damage detectability around the rivets is heavily reduced since the wave propagation will be blocked by the rivet holes.

Since both Fig. 6 and Fig. 7 are only a representation of target function f of Eq. (5) from every pixel, they cannot be scaled on the same level due to different geometrical conditions (e.g.: without hole in Fig. 6 vs rivet holes in Fig. 7). In future work, we plan to make an experimental validation of this approach.

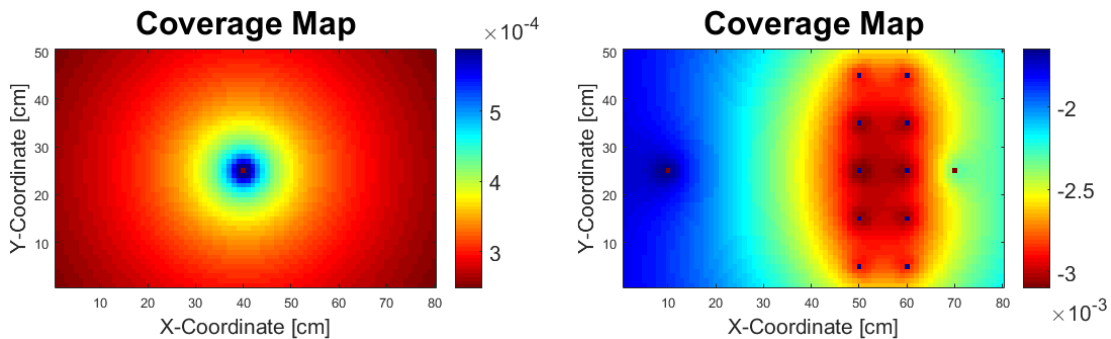


Figure 6: Coverage map based on f -value for sensor placement at (x|y = 40|25 cm) in an 80x50 cm plate

Figure 7: Coverage map based on f -value for sensors placement at (x|y = 10|25 cm) and (x|y = 70|25 cm) in an 80x50 cm plate

CONCLUSION AND OUTLOOK

In this paper, we have proposed a workflow for sensor positioning based on a knowledge of the damage location. An algorithm which can minimize the target function TS will be further developed as a continuation of this project.

REFERENCES

1. Wilcox PD, Dalton RP, Lowe MJS, Cawley P. *Mode and Transducer Selection for Long Range Lamb Wave Inspection*. Journal of Intelligent Material Systems and Structures, 1999. Vol. 12: pp 152 – 161.
2. Ewald V, Ochoa P, Groves RM, Boller C. *Design of a Structural Health Monitoring System for a Damage Tolerance Fuselage Component*. 7th International Symposium of on NDT in Aerospace, Bremen, 2015.
3. Kuznetsov S, Ozolinsh E, Ozolinsh I, Pavelko I, Pavelko V, Wevers M, Pfeiffer H. *Lamb Wave Interaction with a Fatigue Crack in a Thin Sheet of Al2024-T3*. EU Project Meeting on AISHA, Leuven, 2007.
4. Harris CE, Starnes Jr JH, Shuart MJ. *Advanced Durability and Damage Tolerance Design and Analysis Methods for Composite Structures – Lesson Learned from NASA Technology Development Programs*. NASA Langley Research Center, Hampton, 2003.
5. Gilchrist MD. *Attenuation Of Ultrasonic Rayleigh-Lamb Waves By A Symmetrical Embedded Crack In An Elastic Plate*. Journal of Applied Mathematics and Mechanics, 1999. Vol. 79: pp 497 – 498.
6. Wang Q, Su Z. *Crack Diagnosis and Monitoring Method Using Linear-Phased PZT Sensor Array*. Proc. 2nd International Conference of Structural Health Monitoring and Integrity Management, Nanjing, 2014
7. Cobb RG, Liebst BS. *Sensor Placement and Structural Damage Identification from Minimal Sensor Information*. AIAA Journal, 1997. Vol. 35: pp 369 – 374.
8. Shi ZY, Law SS, Zhang LM. *Optimum Sensor Placement for Structural Damage Detection*. Journal of Engineering Mechanics, 2000. Vol. 126: pp 1173 – 1179.
9. Kripakaran P, Saitta S, Ravibndran S, Smith IFC. *Optimal Sensor Placement for Damage Detection*. Proc. 18th International Workshop on Database and Expert System Applications, Regensburg, 2007.
10. Haynes C. *Effective Health Monitoring Strategies for Complex Structures*. PhD Dissertation. University of California San Diego (UCSD), San Diego, 2014.
11. Thiene M, Sharif Khodaei Z, Aliabadi MH. *Optimal Sensor Placement for Maximum Area Coverage for Damage Localization in Composite Structures*. Smart Materials and Structures, 2016. Vol. 25: 095037.
12. Venkat RS, Boller C, Qiu L, Ravi NB, Mahapatra DR, Chakraborty N. *Integrated Approach to Demonstrate Optimum Sensor Positions in a Guided Wave Based SHM System Using Numerical Simulation*. Proc. 8th International Symposium on NDT in Aerospace, Bangalore, 2016.
13. Döring D. *Luftgekoppelter Ultraschall und Geführte Wellen für die Anwendung in der Zerstörungsfreien Werkstoffprüfung*. PhD Dissertation. Universität Stuttgart, Stuttgart, 2011.
14. Pant S. *Lamb Wave Propagation and Material Characterization of Metallic and Composite Aerospace Structures for Improved Structural Health Monitoring (SHM)*. PhD Dissertation. Carleton University, Ottawa, 2014.
15. Hosseini SMH, Gabbert U. *Analysis of Guided Lamb Wave Propagation (GW) in Honeycomb Sandwich Panels*. Proceedings in Applied Mathematics and Mechanics, 2010. Vol. 10: pp 11 – 14.
16. Gomez P, Fernández JP, Garcia PD. *Lamb Waves and Dispersion Curves in Plates and its Applications in NDE Experiences Using COMSOL Multiphysics Pablo Gómez*. Proc. COMSOL Conference, Stuttgart, 2011.
17. Duczek S, Joulaian M, Düster A, Gabbert U. *Numerical Analysis of Lamb Waves Using the Finite and Spectral Cell Methods*. Int. Journal for Numerical Methods in Engineering, 2014. Vol. 99: pp 26 – 53.
18. Cerniglia D, Pantano A, Montinaro N. *3D Simulations and Experiments of Guided Wave Propagation in Adhesively Bonded Multi-Layered Structures*. Journal of NDT & E International, 2010. Vol. 43: pp 527 – 535.
19. Iesulauro E, Ingrassia AR, Arwade S, Wawrzynek PA. *Simulation of Grain Boundary Decohesion and Crack Initiation in Aluminum Microstructure Models*. ASTM Journal of Fatigue and Fracture Mechanics, 2003. Vol. 33: pp 715 – 728.
20. Kanji O, Gallego A. *Attenuation of Lamb Waves in CFRP Plates*. Journal of Acoustic Emission, 2012. Vol. 30: pp 109 – 123.